

Detecting low-pay reservoirs in salt provinces using 3D inversion of marine CSEM surveys—a Gulf of Mexico case study

J.J. Zach (jjz@emgs.com), M.A. Frenkel (mfrenkel@emgs.com), A.M. Ostvedt-Ghazi (amghazi@emgs.com), A. Kumar (akumar@emgs.com), T. Pham (pham@emgs.com)

ABSTRACT

Detection and delineation of reservoirs in the presence of high salt concentrations are recognized as a major challenge to marine controlled-source electromagnetic (CSEM) methods. Using 3D inversion applied to data from a recent grid acquisition, including wide-azimuth data, we demonstrate our ability to resolve a smaller target (2km x 2km) with low-resistivity pay ($\Delta\rho < 5 \Omega\text{m}$) in the vicinity (<1km) of large salt bodies. The inversion is based on an iterative scheme with quasi-Newton update and the use of fast finite-difference time-domain modeling. Using our methodology, we have successfully addressed the client's request to probe the neighborhood of a proven reservoir for similar targets.

Introduction

Marine CSEM surveys have experienced a renaissance in this decade after the invention of Seabed Logging and their application towards hydrocarbon exploration (e.g., Eidesmo et al., 2002). Advances in hardware and operations have resulted in a vast improvement in data quality, permitting the acquisition of well-defined and repeatable grids of seabed receivers with complex towing patterns including the acquisition of wide-azimuth data. Thus, marine CSEM has become a method for 3D imaging of complex geological settings, which is increasingly adopted by the industry, either as a standalone method or in conjunction with other geophysical probes, such as seismic (Norman et al., 2008) or MT (Commer and Newman, 2008). Recent published case studies include Carrazone et al. (2008), Price et al. (2008) and Plessix, van der Sman (2008).

To date, most solutions brought forward to solve the 3D marine CSEM problem rely on an iterative approach with repeated computation of the gradient of a misfit functional with respect to the discrete conductivity grid: $g = \partial \varepsilon / \partial \sigma$, where the L2-norm is the most common choice for the data misfit $\varepsilon = \sum_{s,r,\omega,F} (\text{Weight})(\bar{x}_r | \bar{x}_s; \omega) |\Delta F_i(\bar{x}_r | \bar{x}_s; \omega)|^2$. Differences lie

mainly in the forward operators, the gridding of the forward and/or inversion grid and preconditioning approaches used in the optimization steps. Notable among the most recent contributions on inversion methodology are Commer and Newman (2008) on joint CSEM and MT inversion, as well as Jing et al. (2008), which shows the importance of anisotropy in many surveys. See also the references quoted in Zach et al. (2008a).

The resistivity of geologic salt deposits is found to be well in excess of hydrocarbon reservoirs, while the lateral extent is roughly comparable. Together with the marine CSEM frequency range of ~0.1-10 Hz impeding the differentiation of resistivities beyond $\sim 10^2 \Omega\text{m}$, that has been rendering the detection of hydrocarbons in the presence of large concentrations of salt a major challenge. We were recently approached by Focus Exploration, LLC, a Gulf of Mexico (GoM) prospect generation company, to examine an area in the GoM with large concentrations of salt for possible hydrocarbon-bearing prospects in the vicinity of an existing and proven reservoir. In this study, we present 3D inversion of a receiver grid which includes the know reservoir as a calibration target.

Methodology

The 3D case study presented here was inverted following Zach et al. (2008a), using a quasi-Newton method, where the inverse Hessian is approximated by an outer product formulation of the vectors of an integer number of past iterations' update steps and gradient changes (following Byrd et al., 1995). The forward problem is solved with the finite-difference time-domain solver described in Maaø, F. A. (2007), and the gradient is calculated at each iteration using a Green's function approach (Støren et al., 2008), based on the assumption of the first Born-approximation applied to the difference field between synthetic and real data.

The data from the grid shown in figure 1 (left) was conditioned for 3D inversion, producing frequency-domain data and noise estimates using the methodology described in Zach et al. (2008b). The source-signature was designed to have the transmitted energy concentrated on four main frequency modes: 0.25, 0.5, 0.75 and 1.0Hz. While towing the source over each receiver was still necessary to accurately determine its orientation, azimuthal data could be recovered which is accurate to within 5% in magnitude and 5 degrees in phase.

As a pre-stage to full 3D inversion, plane-layer inversions of several or all receivers are run to identify general trends and to determine a starting model. A plane-layer simulated-annealing scheme (Roth and Zach, 2007) is used to invert individual receiver data for 2-3 frequencies and for the Ex- and Hy-fields simultaneously. The depth is discretized using a

stretched grid with 30-100 bins from mudline, and using an exponential cooling scheme, convergence is typically reached after 10^4 iterations (a few hours on a single processor).

The 3D inversion proceeds in the iterative loop shown in figure 1 (right), where the input consists of the starting model and the conditioned data and weights. Using the estimated noise at each frequency mode, a binary weighting scheme is employed with a SNR-cutoff of 24 dB. Data preconditioning and a gradient muting approach to minimize acquisition imprints, are described in Zach et al. (2008a). Due to better noise suppression compared to magnetic data, only the electric field was used in the inversion, whereas inline and azimuthal data from next-neighboring lines were included, and data convergence to within measurement accuracy is achieved within 80-200 iterations (about 1 week on 150 parallel nodes).

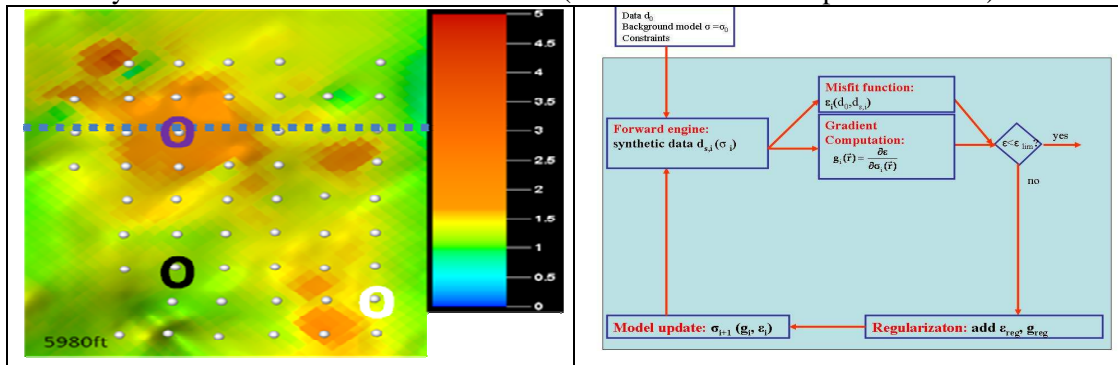


Figure 1: Left: 3D grid of receiver locations (representative, and specifically used here) for 3D inversion with 900m receiver spacing; shown is the resistivity map from full 3D inversion at a certain reservoir depth slice; the top salt horizon which is the subject of this study is located at greater depths. Right: iterative loop for Hessian-based 3D inversion (from Zach et al., 2008a).

Case study

Figure 2 shows results from three plane-layer inversions, in which data convergence was achieved after 10000 simulated-annealing cooling steps. For shorter offsets, where the plane layer inversion result is more reliable, resistivities between 1.5-3 Ωm are observed, which are associated with layers of relatively resistive shale. Beyond 600-800 m below mudline, a conductive layer is recovered, which is associated with brine-saturated sandstone. At depths greater than 1.3-2 km below mudline, the resistivity gradually increases, signifying the appearance of salt.

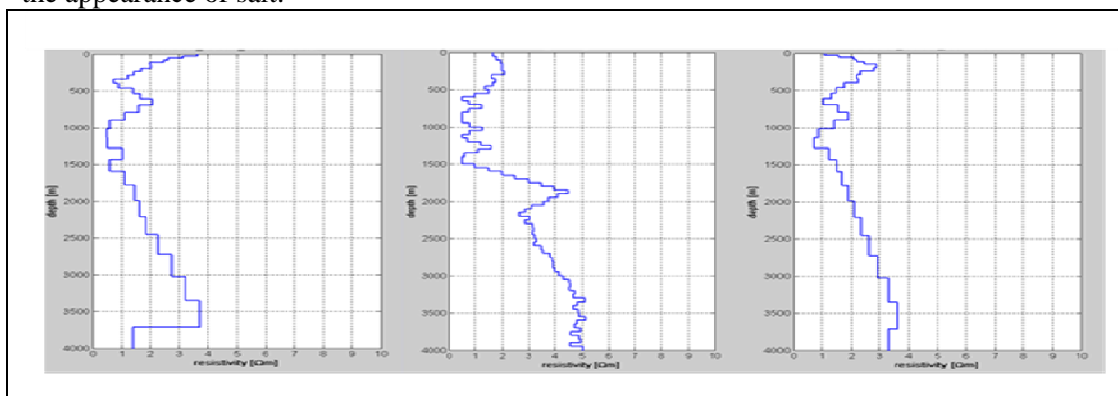


Figure 2: Plane-layer inversion of the receiver indicated as a black (left), purple (center) and white (right) circle in figure 1, using a simulated annealing- approach.

The results from plane-layer inversion were used to build starting models for full 3D inversion. Using the average resistivity obtained for the first 500m, a $2\Omega\text{m}$ -halfspace model was first used to avoid any bias. The inversion of the four dominant frequencies, projected on one grid line, is shown in figure 3, confirming the overall geology known from 3D-seismics and well-control. While the hydrocarbon reservoir is recovered from the unbiased inversion, seismic data and geologic knowledge of the shale overburden are needed for identification.

The proven reservoir is known from both 3D seismics and well control (the well log still being confidential) to be a ~2km x 2km- resistor with stacked, low-resistivity pay (4-5 Ωm), which is recognized as a challenging EM-target. In order to improve the quality of its imaging, a complex initial model is used in a second 3D inversion, which exploits the certainty concerning the shales and the conductive sands below, which is evident from inverted CSEM data only. The initial resistivity linearly decreases from 2 Ωm to 1 Ωm from mudline to 500 m depth, below which a 1 Ωm-halfspace is used. The shielding effect of the latter prevents salt from perturbing the reservoir image. The result is shown in figure 4, along with the seismic image and the known stacked pay zones, the depths of which are reproduced to within the resolution of the CSEM method (~10% of the burial depth).

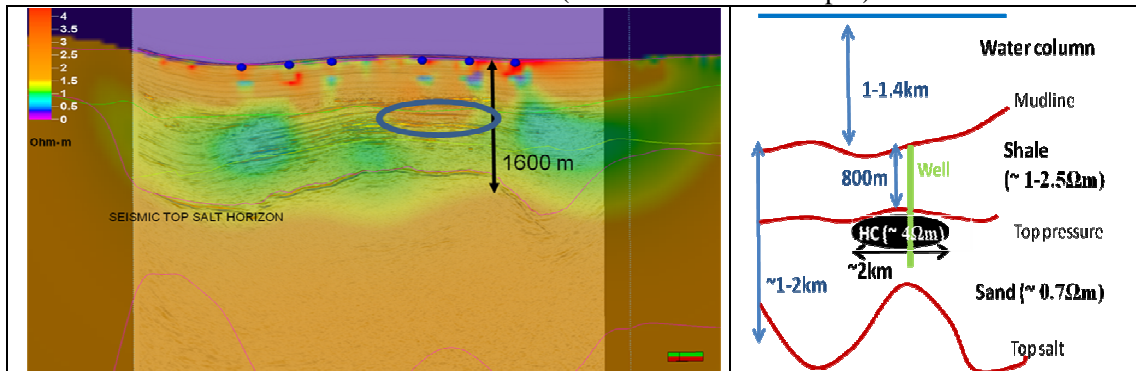


Figure 3: Left: projection of the resistivity cube from the final unbiased 3D inversion onto the dashed line on figure 1, overlaid with a 3D seismic-image, along with the interpreted seismic top-salt horizon. The top-salt horizon is recovered to within 50-150 m, whereas most of the deviation occurs below the proven hydrocarbon reservoir. Features in the subsurface known from well control and extensive seismic data, including the brine-saturated sandstone and the shale in shallow regions, are also recovered (right). However, the hydrocarbon reservoir (blue oval on the left) is only imaged with good quality with subsequent analysis.

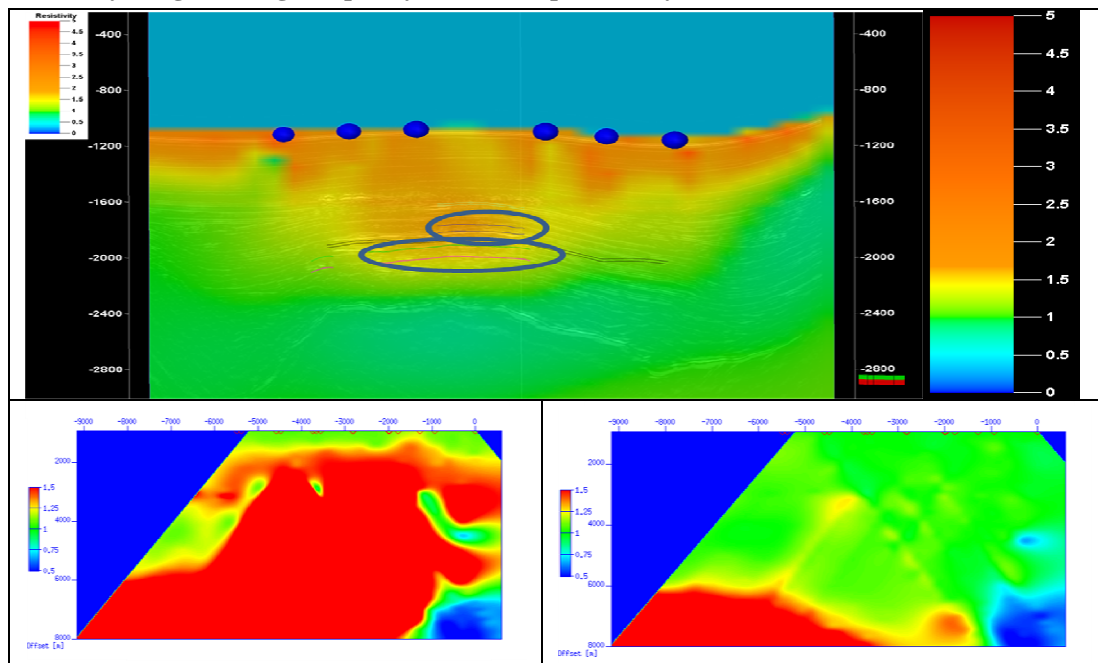


Figure 4: Projection of the final resistivity cube for 3D inversion with a complex starting model onto the dashed line in figure 1, overlaid with a 3D seismic-image, as well as known stacked pay zones (blue ovals, encompassing a total of five zones). Bottom left (right): data misfit for initial (final) model in magnitude for the f=0.5 Hz-mode, showing convergence to within the measurement accuracy (representative for magnitude and phase for all frequencies). All remaining data misfit is associated with the salt structures at greater depths.

Conclusions

Using 3D acquisition grids and gradient-based 3D inversion methods, we have demonstrated the applicability of marine CSEM methods to image a known reservoirs in the close vicinity (<1km stacking) of complex salt structures. Thereby, we have responded to the client's request, which was to seek similar reservoirs to the known pay in the same prospect. This implies the basic applicability of CSEM/SBL to "salt provinces" such as the GoM.

Acknowledgements

We thank the geoscientists of Focus Exploration, LLC, for valuable discussions as well as the agreement to show these data. We further would like to thank EMGS ASA for supporting this study and permitting its publication.

References

- Byrd, R.H., Lu, P., Nocedal, J. (1995) A Limited Memory Algorithm for Bound Constrained Optimization. *SIAM Journal on Scientific and Statistical Computing*, 16, 5, 1190-1208.
- Carrazone, J.J., Dickens, T.A., Green, K.E., Jing, C., Wahrmund, L.A., Willen, D.E., Commer, M., Newman, G.A. (2008) Inversion study of a large marine CSEM survey. *SEG 2008 Expanded Abstracts*, Las Vegas, NV, USA.
- Commer, M., Newman, G.A. (2008) Optimal conductivity reconstruction using three-dimensional joint and model-based inversion for controlled-source and magnetotelluric data, *SEG 2008 Expanded Abstracts*, Las Vegas, NV, USA.
- Eidesmo, T., Ellingsrud, S., MacGregor, L.M., Constable, S., Sinha, M.C., Johansen, S., Kong, F.N. and Westerdahl, H. (2002) Sea Bed Logging (SBL), a new method for remote and direct identification of hydrocarbon filled layers in deepwater areas. *First Break*, 20, 144-152.
- Jing, C., Green, K.E., Willen, D.E. (2008) CSEM inversion: Impact of anisotropy, data coverage, and initial models. *SEG 2008 Expanded Abstracts*, Las Vegas, NV, USA.
- Maaø, F. A. (2007) Fast finite-difference time-domain modeling of marine-subsurface electromagnetic problems. *Geophysics*, 72(2), A19-A23.
- Norman, T., Alnes, H., Christensen, O., Zach, J.J., Eiken, O., Tjøland, E. (2008) Planning Time-lapse CSEM-surveys for Joint Seismic-EM Monitoring of Geological Carbon Dioxide Injection. *EAGE Budapest 2008 CO2 Geological Storage Workshop*.
- Plessix, R.-E., van der Sman, P. (2008) Regularized and blocky controlled source electromagnetic inversion. *PIERS 2008*, Cambridge, Mass.
- Price, A., Turpin, P., Erbetta, M., Watts, D., Cairns, G. (2008) 1D, 2D and 3D modeling and inversion of 3D CSEM data offshore West Africa. *SEG 2008 Expanded Abstracts*, Las Vegas, NV, USA.
- Roth, F., Zach, J.J. (2007) Inversion of marine CSEM data using up-down wavefield separation and simulated annealing. *SEG 2007 Expanded Abstracts*, San Antonio, TX, USA.
- Støren, T., Zach, J.J., Maaø, F. (2008) Gradient calculations for 3D inversion of CSEM data using a fast finite-difference time-domain modelling code, *EAGE 2008 Expanded Abstracts*, Rome, Italy.
- Zach, J.J., Bjørke, A.K., Støren, T., Maaø, F. (2008a) 3D inversion of marine CSEM data using a fast finite-difference time-domain forward code and approximate Hessian-based optimization. *SEG 2008 Expanded Abstracts*, Las Vegas, NV, USA.
- Zach, J.J., Roth, F., Yuan, H. (2008b) Data preprocessing and starting model preparation for 3D inversion of marine CSEM surveys. *EAGE 2008 Expanded Abstracts*, Rome, Italy.